Solid-State NMR and Diffraction Studies of a Tunable *p-tert*-Butylcalix[4]arene·Guest Structure§

E. B. Brouwer,†,‡ G. D. Enright,† and J. A. Ripmeester*,†,‡

Contribution from the Steacie Institute for Molecular Science, National Research Council of Canada, Ottawa, Ontario, Canada K1A 0R6, and Ottawa-Carleton Chemistry Institute, Department of Chemistry, Carleton University, 1125 Colonel By Drive, Ottawa, Ontario, Canada K1S 5B6

Received October 30, 1996⊗

Abstract: The majority of *p-tert*-butylcalix[4]arene inclusion compounds are 4-fold symmetric in the solid state, with the guest molecular and the host symmetry axes approximately aligned. In contrast, nitrobenzene (and related guests) induces a permanent symmetry-reducing distortion of the *p-tert*-butylcalix[4]arene compound and occupies a position in which the guest molecular axis is no longer aligned with that of the host. These compounds have been characterized by single-crystal X-ray diffraction as well as ^{13}C CP-MAS and ^{2}H NMR in the solid state. Introduction of propane as a second, minority guest in sufficient quantities induces the alignment of the nitrobenzene molecular axis with the host C_4 symmetry axis. Nitrobenzene-d_5 guest dynamics in the symmetric and asymmetric structures reveal a much stronger host·guest interaction in the latter. The nature of the asymmetry is due to a cooperative effect rather than any intrinsic property of the individual *p-tert*-butylcalix[4]arene·guest units. In general, this work give initial insight into the suitability of the *p-tert*-butylcalixarene[4]arene framework for crystal engineering and illustrates the close connection between dynamics and lattice symmetry and structure.

Introduction

In light of the fact that a large number of solid-state *p-tert*-butylcalix[4]arene (tBC) inclusions have 4-fold symmetry and that the toluene compound[1] and perhaps others are now known to be 4-fold symmetric only on time average, this paper reports attempts to induce permanent asymmetry into the tBC structure, and to understand the nature of the distortion. In a short communication we have reported that in contrast to the similarly-shaped toluene guest, nitrobenzene occupies an asymmetric tBC cavity with the guest molecular axis far from the host symmetry axis and the guest's ring substitutent points out of—rather than into—the cavity.[2] The lattice can be tuned back into a symmetric form by the introduction of a co-guest in sufficient quantity. This links the asymmetry to a cooperative intermolecular effect rather than any intrinsic property of the individual calixarene·-guest unit. Guest dynamics in the symmetric and asymmetric forms of the tBC confirm the much stronger host·guest interaction in the latter. In a broader context, this work provides insight into the suitability of the tBC lattice for crystal engineering based on weak, nonbonding intermolecular interactions, and suggests that it may be possible to produce "pillared" forms of tBC suitable for gas adsorption.

Despite the variety of possible conformations, most alkylcalix-[4]arenes prefer the 4-fold symmetric cone conformation in the solid state (especially when the rim modifications are minimal) as is evident from structural[3,4] and modeling studies.[5] Preference for the 4-fold symmetric conformation of the simple tBC is remarkable considering the variety of guest molecules it is known to include.[6] Distortion of the host cavity is expected to occur given an appropriate guest; the distinctiveness may arise from such factors as guest shape and electronic charge density. Chiral selectivity of *p*-sulfonatocalix[*n*]arenes toward chiral guests in solution does hint that the calixarene cavity can distort to recognize specific guest shapes.[7] Structural and dynamic studies of *p-tert*-butylcalix[4]arene·toluene suggest that the high observed symmetry results from space-averaging of a cavity which has only 2-fold symmetry.[1] Finally, gas-phase modeling studies indicate that the calixarene host adopts a C_{2v} elliptical rather than a C_4 conical geometry,[8] a feature that has also been observed for [alkyl]calix[4]arene in solution.[9]

Solid-State NMR Spectroscopy. ^{13}C NMR in the solid state (with cross-polarization (CP) and magic angle spinning (MAS)) gives spectra that are similar to those obtained in solution. However, in the solid state, chemical shift differences may arise from chemically equivalent but crystallographically inequivalent nuclei, and the ^{13}C NMR spectra give information on the content

§ NRCC No. 40822.

† National Research Council of Canada.

‡ Carleton University.

⊗ Abstract published in *Advance ACS Abstracts,* May 15, 1997.

(1) Brouwer, E. B.; Enright, G. D.; Ratcliffe, C. I.; Ripmeester, J. A. *Supramol. Chem.* **1996**, *7*, 79−83. Brouwer, E. B.; Ripmeester, J. A.; Enright, G. D. *J. Inclusion Phenom.* **1996**, *24*, 1−17.

(2) Brouwer, E. B.; Enright, G. D.; Ripmeester, J. A. *Supramol. Chem.* **1996**, *7*, 7−9.

(3) Andreetti, G. D.; Ungaro, R.; Pochini, A. *J. Chem. Soc., Chem. Commun.* **1979**, 1005−1007. Furphy, B. M.; Harrowfield, J. M.; Ogden, M. I.; Skelton, B. W.; White, A. H.; Wilner, F. R. *J. Chem. Soc., Dalton Trans.* **1989**, 2217−2221. Harrowfield, J. M.; Ogden, M. I.; Richmond, W. R.; Skelton, B. W.; White, A. H. *J. Chem. Soc., Chem. Commun.* **1991**, 1159−1161. Xu, W.; Puddephatt, R. J.; Manojlovic-Muir, L.; Muir, K. W.; Frampton, C. S. *J. Inclusion Phenom.* **1994**, *19*, 277−290.

(4) Ungaro, R.; Pochini, A.; Andreetti, G. D.; Domiano, P. *J. Chem. Soc., Perkin Trans. 2* **1985**, 197−201.

(5) Minn, H. H.; Chang, S.; No, K. T. *Theor. Chim. Acta* **1989**, *75*, 233−245. Drew, M. G. B. In *Spectroscopic and Computational Studies of Supramolecular Systems*; Davies, J. E., Ed.; Kluwer: Dordrecht, 1992; pp 207−237.

(6) Gutsche, C. D. *Calixarenes*; RSC: Cambridge and London, 1989. Vicens, J.; Bohmer, V., Eds. *Calixarenes*; Kluwer: Dordrecht, 1990. Ungaro, R.; Arduini, A.; Casnati, A.; Ori, O.; Pochini, A.; Ugozzoli, F. In *Computational Approaches in Supramolecular Chemistry*, Wipff, G., Ed.; NATO ASI Series, C426; 1994; pp 277−300. Bohmer, V. *Angew. Chem., Int. Ed. Engl.* **1995**, *34*, 713−745.

(7) Morozumi, T.; Shinkai, S. *J. Chem. Soc., Chem. Commun.* **1994**, 1219−1220.

(8) Grootenhuis, P. D. J.; Kollman, P. A.; Groenen, L. C.; Reinhoudt, D. N.; van Hummel, G. J.; Ugozolli, F.; Andreetti, G. D. *J. Am. Chem. Soc.* **1990**, *112*, 4165−4176. Guilbaud, P.; Varnek, A.; Wipff, G. *J. Am. Chem. Soc.* **1993**, *115*, 8298−8312.

(9) Conner, M.; Janout, V.; Regen, S. L. *J. Am. Chem. Soc.* **1991**, *113*, 9670−9671.

S0002-7863(96)03776-6 CCC: $14.00 Published 1997 by the American Chemical Society

of the smallest repeat unit in the crystal. Solid-state NMR spectroscopy is sensitive to short-range ordering whereas single-crystal X-ray diffraction techniques depend on lattice symmetry and hence long-range ordering. We use both techniques in a complementary fashion to establish structural and dynamic features.

A thorough treatment of the background to solid-state NMR spectroscopy has been published,[10] and a brief summary of the pertinant theory for ^{2}H NMR is presented below. The quadrupolar coupling interaction, which dominates the line shapes of solid-state ^{2}H NMR spectra, is exceedingly sensitive to molecular motions in the range of $\kappa = 10^4-10^7$ Hz which significantly modify the shape of the powder line shape. The appropriate parameters to model dynamic states are obtained from these spectra. The motional effects can be grouped into three categories based on the motional rate:

(a) Slow Motions ($\kappa < 10^4$ Hz). The motions occur on a time scale much greater than the quadrupolar coupling interaction ν_Q^{-1} ($\sim 10^4$ s^{-1}) and have minimal effects on the ^{2}H NMR line shape. The resulting spectrum is known as the static line shape. There is essentially no reorientation of the electric field gradient (EFG) tensor during the course of the quadrupolar echo measurement.

(b) Intermediate Rate Motions ($\kappa = 10^4-10^7$ Hz). These motions occur on a time scale of the same order as ν_Q^{-1} (10^4-10^7 s^{-1}) and have a profound effect on the observed line shape. The line shapes are very sensitive, both in shape and intensity, to the spacing between the pulses in the quadrupolar echo experiment as well as the rate and mechanism of the molecular motion. The intermediate rate spectra can be simulated in order to confirm a mechanism of a particular molecular motion and to determine its rate. Spectra collected as a function of temperature can be matched to those simulated as a function of the motional rate κ and an Arrhenius plot constructed to determine the activation barrier to the motion.

(c) Fast Molecular Motions ($\kappa > 10^7$ Hz). These motions occur on a time scale much shorter than ν_Q^{-1} ($>10^7$ s^{-1}) and give spectra of reduced width (between the pair of features) compared to static spectra. These spectra are characterized by an effective EFG tensor, and are insensitive to the motional rates. The fast motion limit (FML) spectra may be used to determine possible mechanisms for the molecular motions. Analytical expressions for the parameters governing the line shapes are relatively easy to obtain.[10]

Experimental Section

p-tert-Butylcalix[4]arene·nitrobenzene (tBC·NB) crystallizes from a solution of tBC in warm (80−100 °C) nitrobenzene;[2] tBC·3-nitrotoluene is prepared in a similar fashion. To form tBC·NB·propane, a saturated solution of tBC in nitrobenzene is cooled to room temperature in a closed vessel which is pressurized with the gas (1−12 atm). tBC·propane (no nitrobenzene guest) is prepared by stirring tBC in liquid propane (4 mL) for 1 h, then warming to ambient temperatures to drive off excess propane. A small fraction of tBC units have unoccupied cavities as evident from signals of the empty tBC in the ^{13}C CP-MAS NMR spectrum. 4-Nitrotoluene (mp 53 °C) forms an inclusion compound with tBC when a stoichiometric mixture of the two solids is heated at 100 °C for 1 day.

^{13}C NMR spectra were collected on CXP-180 (45.3 MHz) or AMX-300 (75.3 MHz) Bruker spectrometers by using a cross-polarization pulse sequence with phase cycling and the following probes: Doty 7 mm MAS (45.3 MHz), Doty 7 mm MAS (75.3 MHz), or Bruker 5 mm MAS (75.3 MHz) probes. For collection details, see the figure captions. The samples were referenced to hexamethylbenzene (δ_{Me} = 16.9 ppm). Dipolar-dephased spectra were obtained with use of a 40-μs interruption of proton decoupling before data acquisition; by allowing the magnetization to be dephased briefly by ^{1}H−^{13}C dipolar interactions, the signals due to carbons with strong dipolar couplings to protons (rigidly held in the crystal lattice) disappear, while those of carbons with weak dipolar couplings (quaternary carbons and proton-bearing carbons involved in molecular motion) persist.[11] The quadrupolar echo pulse technique with phase cycling[12] was used to collect the ^{2}H spectra at 46.1 MHz on a Bruker AMX-300 spectrometer (150−300 transients; interpulse delay = 35 μs; recycle time = 10 s; 90° pulse = 2.9 μs) equipped with a Bruker solenoid probe equipped with a 5-mm coil. Spectral simulations of motions at intermediate rates were carried out with the MXET1 FORTRAN program of Vold *et al.*[13]

Table 1. Summary of *p-tert*-Butylcalix[4]arene·Guest Compounds: Structure and Characterization Techniques

material[a]	symmetry	guest position	XRD	^{2}H NMR	^{13}C NMR
α-tBC·NB	C_1	non-axial	yes	yes	yes
tBC·3NT	C_1	non-axial[b]			yes
tBC·4NT	C_2	axial			yes
α-tBC·NB·PROP	C_1	non-axial			yes
β-tBC·NB·PROP	C_4	axial	yes	yes	yes
tBC·PROP	C_4	axial			yes
β-tBC·NB	C_4	axial			yes

[a] tBC = *p-tert*-butylcalix[4]arene; NB = nitrobenzene; PROP = propane; 3NT = 3-nitrotoluene; 4NT = 4-nitrotoluene; α and β indicate the two different structural isomers of tBC·NB; α = non-axial nitrobenzene guest, β = axial nitrobenzene guest. [b] Two guest orientations for tBC·3NT.

Results and Discussion

The structure of tBC·guest compounds has been examined with both X-ray diffraction (XRD) and solid-state NMR techniques (Table 1). We correlate the NMR and XRD data with two different structures, and this provides a basis to be able to deduce structural features from NMR data for which there are no XRD data.

(a) Structure of *p-tert*-Butylcalix[4]arene·Nitrobenzene (α-tBC·NB). Since two orientations of the nitrobenzene guest in the host cavity will be discussed, the prefixes α and β indicate the off-axial and on-axial nitrobenzene orientations, respectively. The ^{13}C CP-MAS NMR spectrum of α-tBC·NB (Figure 1) differs significantly from that typically observed for 4-fold symmetric conical tBC·guest compounds. Whereas the tBC·-toluene spectrum shows a single resonance for each of the four symmetry-related *p-tert*-butylphenol carbons,[1] the α-tBC·NB spectrum shows a multiplicity of up to four for each *p-tert*-butylphenol carbon: this is most clearly visible for the host carbon 7 (δ 33.8−35.1 ppm). The multiplicity indicates a lowering of tBC symmetry from the corresponding 4-fold symmetric tBC·toluene structure. The lines from nitrobenzene carbons 4′ (δ = 134.7 ppm), 3′ (δ = 126.1 ppm), and 2′ (δ = 122.7 ppm) are visible whereas carbon 1′ lies under the host carbon 1 resonance (δ = 146 ppm). In the dipolar-dephasing NMR experiment,[11] some carbon resonances (host 3, 5, and 9; guest 4′) disappear while the remaining guest carbon signals persist. The persistence of the nitrobenzene carbon 2′ and 3′ signals under dipolar-dephasing conditions suggests that these C−H dipolar couplings are averaged by molecular motion whereas the disappearance of the 4′ signal indicates the para-carbon C−H coupling remains intact. The picture of guest motion that emerges is one where the guest undergoes large-

(10) Facey, G. A.; Ratcliffe, C. I.; Ripmeester, J. A. *J. Phys. Chem.* **1995**, *99*, 12249−12256.
(11) Opella, S. J.; Frey, M. H. *J. Am. Chem. Soc.* **1979**, *101*, 5854−5856. Alemany, L. B.; Grant, D. M.; Alger, T. D.; Pugmire, R. J. *J. Am. Chem. Soc.* **1983**, *105*, 6697−6704.
(12) Davis, J. H.; Jeffrey, K. R.; Bloom, M.; Valic, M. I.; Higgs, T. P. *Chem. Phys. Lett.* **1976**, *42*, 390−394.
(13) Greenfield, M. S.; Ronemus, A. D.; Vold, R. L.; Vold, R. R.; Ellis, P. D.; Raidy, T. E. *J. Magn. Reson.* **1987**, *72*, 89−107.

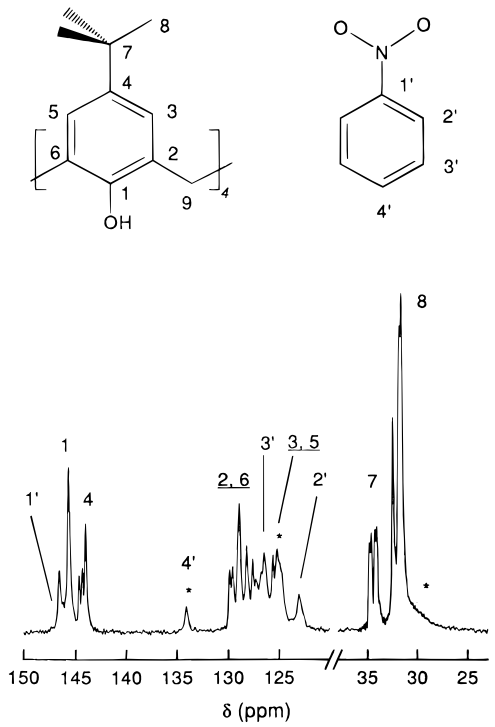

Figure 1. 45.3-MHz ^{13}C CP-MAS NMR spectrum of α-tBC·NB; * = signals that disappear under dipolar dephasing. Collection details: 1500 transients; recycle time = 3.5 s; $\pi/2$ pulse = 2.8 μs; contact time = 3.5 ms; 4K datum points acquired and zero-filled to 16K before processing; ν = 2.86 kHz.

amplitude motion with the C4′−H bond on the symmetry axis for this motion.

A representation of the asymmetric unit of α-tBC·NB is shown in Figure 2a, and the structural details summarized in Table 2 and 3. The axis of the host molecule lies along the *z*-direction with host molecules facing each other in layers with open cavities (Figure 3). Each *p-tert*-butylphenol moiety in the calixarene molecule is unique, and this is consistent with the NMR data. The *tert*-butylphenol subunits, labeled A−D sequentially around the calix with A containing O1, B containing O2, C containing O3, and D containing O4, make dihedral angles with the horizontal plane defined by the four phenolic oxygens of the host ranging from 51.8 to 57.8°. The NO_2 group extends outward from the calixarene axis between subunits A and D.

Two (B, C) of the four *p-tert*-butylphenol subunits display a positional disorder with site occupancies of 0.57:0.43 (B) and 0.79:0.21 (C). In contrast to that of the tBC·toluene structure,[1] the *tert*-butylphenol positional disorder ratio is not readily related to the guest position. The *p-tert*-butylphenol site occupancies likely arise from subtle interactions between the nitrobenzene in the nearest adjacent calix cavity. The packing diagram (Figure 3) shows that the *ab* layers of calixarenes are stacked in a staggered or shifted fashion compared to the layers in tBC·-toluene. The shift of the *ab* layers results in a loss of crystal symmetry, which is manifested in a doubling of *c* to 26.7560 Å and a change in the space group to orthorhombic ($Pc2_1n$) from tetragonal ($P4/n$). Instead of one calix being capped equally by four calix cavities in the next layer above as in C4A·-toluene, three tBC's shift to minimize the *p-tert*-butyl···-nitrobenzene interaction while the fourth tBC shifts closer to the guest. It is the *tert*-butyl group of the fourth calix (*tert*-butyl disorder 0.57:0.43) that interacts strongly with the nitrobenzene (CN2···Me = 3.39 Å; Σ van der Waals (vdW) radii = 3.6 Å). The *p-tert*-butylphenol disorder in this case

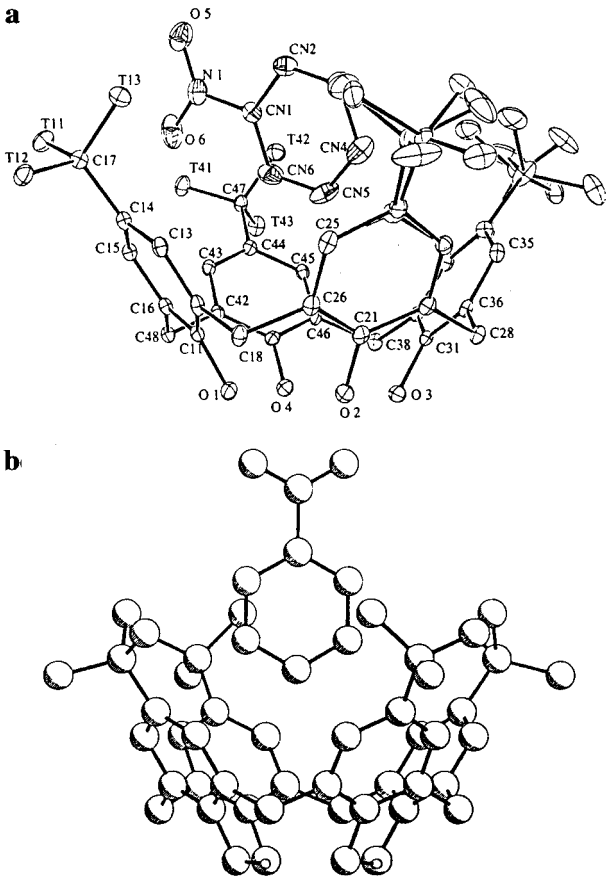

Figure 2. ORTEP plot of α-tBC·NB (a) and PLUTO plot of β-tBC·-$NB_{0.64}$·$PROP_{0.36}$ (b, major guest only). The labeling of the host and guest in β-tBC·$NB_{0.64}$·$PROP_{0.36}$ is the same as in α-tBC·NB. Hydrogen atoms are omitted for clarity.

arises more from the interactions with the guest in adjacent layers than from the interactions with the resident guest.

The absence of disorder in two of the *p-tert*-butylphenol units (A, D) may be related to the nitrobenzene off-axis position (and specifically the nitro group being sandwiched between the two ordered *p-tert*-butyl groups), which induces a degree of "stiffness" in the flexible tBC framework. In symmetric tBC cavities, the guest, which lies on or very near the compound symmetry axis, is dynamic and carves out a volume of occupation that is axially symmetrical as a result of fast guest motion; however, the volume is not symmetrical when the guest is static. The α-tBC·NB structure shows a guest restricted in its motion; the guest presents an asymmetric shape (particularly the nitro group) to the calix cavity, which enclathrates the guest in a manner that may lock in and order the two *p-tert*-butyl groups.

Some striking aspects of the structure are the off-axis position of the guest and the absence of guest disordering. The C_2 axis of the planar (within 0.1 Å) nitrobenzene is 67.9° off the *z*-axis (perpendicular to the plane defined by the four phenolic oxygens); in symmetric tBC·guest structures, the calix and guest molecular axes aligned within 10°. The center of the nitrobenzene ring is close (0.24 Å) to the axis of the host. The plane of the nitrobenzene makes an angle of 68.8° with the basal plane defined by the four hydrogen-bonded host oxygens.

The points where the guest and host interact are pertinent to the origin of the guest-induced calix distortion. The interlayer interaction between the guest CN2 and the *p-tert*-butyl methyl has been noted above; equally important are the intramolecular interactions, *i.e.*, those between the guest and its host cavity. The *D p-tert*-butylphenol moiety seems to play the most important role: the nitrobenzene sits nearly perpendicular to

Table 2. Crystallographic Data for α-tBC·Nitrobenzene and β-tBC·Nitrobenzene$_{0.64}$·Propane$_{0.36}$[a]

compound	α-tBC·NB	β-tBC·NB$_{0.64}$·PROP$_{0.36}$
formula	$C_{50}H_{61}NO_6$	$C_{12.23}H_{15.55}N_{0.16}O_{1.32}$
fw	771.91	185.93
temperature, K	150	150
color	colorless	colorless
crystal size, mm	0.35 × 0.20 × 0.12	0.15 × 0.25 × 0.30
crystal system	orthorhombic	tetragonal
space group	$Pc2_1n$	$P4/n$
a, Å	12.4355(4)	12.946(11)
b, Å	12.9346(5)	12.946(11)
c, Å	26.7560(12)	12.568(10)
V, Å^3	4303.7(3)	2106.3
Z	4	8
ρ_{calc}, g cm^{-3}	1.191	1.173
$F(000)$	1668.42	807.1
μ(Cu Kα) mm^{-1}	0.57	0.55
scan type	$\theta/2\theta$	$\theta/2\theta$
data collected	h, k, l	h, k, l
$2\theta_{max}$, deg	140	140
total no. of reflcns	5465	4113
no. of unique reflcns	5377	2008
R_{merge}	0.030	0.039
no. of reflcns $I \geq 2.5\sigma(I)$	5095	1313
no. of variables	556	178
R	0.041	0.124
R_w	0.057	0.167
GOF	2.14	5.76
max Δ/σ (final cycle)	0.077	0.049
residual density, e Å^{-3}	−0.290 to 0.220	−0.36 to 0.39

[a] Single-crystal X-ray diffraction was carried out at 150 K on an Enraf-Nonius CAD4 diffractometer using the NRCVAX suite of programs; $\lambda = 1.54056$ Å. A graphite monochromator with an aperture of 4.0 × 4.0 was at a distance of 173 mm from the crystal. Stationary background counts were collected at each end of the scan (scan/background time ratio 5:1) and peak and background counts were determined with the profile analysis procedure found in: Gabe, E. J.; Le Page, Y.; Charland, J.-P.; Lee, F. L.; White, P. S. *J. Appl. Crystallogr.* **1989**, *22*, 384−387. $\sigma(F_o)$ is based on counting statistics, function minimized $\sum w(|F_o| - |F_c|)^2$, where $w = [\sigma^2(F_o) + k(F_o)^2]^{-1}$, $R = \sum||F_o| - |F_c||/\sum|F_o|$, $R_w = (\sum w(|F_o| - |F_c|)^2/\sum w|F_o|^2)^{1/2}$, and GOF $= [\sum w(|F_o| - |F_c|)^2/(m - n)]^{1/2}$. Values given for R, R_w, and GOF are based on those reflections with $I \geq 2.5\sigma(I)$.

the *p-tert*-butylphenol aromatic ring (100.3°), and is close to the geometry of T- or edge-to-face (rather than $\pi-\pi$ stacking) aromatic interactions which have been identified as stabilizing interactions between aromatic rings.[14] The guest CN6 makes significant contacts with the phenol C42 and C43: 3.52 and 3.62 Å ($\sum r_{vdW} = 3.6$ Å); this includes the hydrogen of the CN6−H bond of the guest which is directed towards the bond between C42 and C43.

The oxygen pointing towards the cavity (O6) interacts with the methyls of *p-tert*-butylphenol groups A (T11) and D (T41) and makes contacts of 3.66 and 3.48 Å, respectively ($\sum r_{vdW} = 3.6$ Å). The second oxygen (O5) points out of the cavity and interacts with T13 and T41 of the *tert*-butyl methyls of *p-tert*-butylphenol groups A and D: 3.69 and 3.70 Å; the shortest contact with the above *tert*-butylmethyl group (T12) is comparable (3.68 Å). The two N−O bond lengths are not exactly equal: N−O6 is slightly longer (1.238 Å) than N−O5 (1.217 Å); the difference may arise from a CH···O interaction, which is stronger for the longer N−O bond. These parameters quantify the nature of the compound asymmetry, which originates from the steric requirements of the nitro group.

The unsubstituted end of the nitrobenzene molecule interacts with the disordered *p-tert*-butylphenol methyl groups, both in the host calix and the adjacent units. This end of the guest is not as tightly anchored as the nitro end and undergoes some motion as indicated by the larger thermal parameters of the carbons CN3, CN4, and CN5 (Figure 2). The observed positional disorder in the *p-tert*-butylphenol groups may be related to the nitrobenzene motion.

(14) Hunter, C. A. *Chem. Rev.* **1994**, 101−109. Paliwal, S.; Geib, S.; Wilcox, C. S. *J. Am. Chem. Soc.* **1994**, *116*, 4497−4498.

Table 3. Final Positional and Equivalent Isotropic Thermal Parameters (Å^2) for α-tBC·NB

atom	x	y	z	B_{iso}[a]
O 1	0.76876(14)	0.98149	0.22971(6)	1.91(7)
C11	0.81668(19)	1.0125(3)	0.27404(10)	1.49(9)
C12	0.79542(20)	1.11092(25)	0.29322(10)	1.61(9)
C13	0.85038(20)	1.1420(3)	0.33574(10)	1.61(10)
C14	0.92558(19)	1.0791(3)	0.35966(10)	1.62(9)
C15	0.94181(20)	0.9797(3)	0.34000(9)	1.57(9)
C16	0.88737(19)	0.94472(25)	0.29750(10)	1.47(9)
C17	0.98821(21)	1.1230(3)	0.40454(10)	1.74(10)
C18	0.71386(21)	1.1837(3)	0.26910(10)	1.72(9)
O 2	0.56331(14)	1.04462(22)	0.22662(7)	2.01(7)
C21	0.53081(20)	1.0968(3)	0.26916(9)	1.59(9)
C22	0.42852(20)	1.08026(25)	0.28963(10)	1.59(9)
C23	0.39866(20)	1.1392(3)	0.33095(10)	1.67(9)
C25	0.56769(21)	1.2249(3)	0.33144(10)	1.89(10)
C26	0.60153(20)	1.1687(3)	0.28987(10)	1.69(9)
C28	0.35236(20)	0.9988(3)	0.26905(10)	1.59(9)
O 3	0.49369(14)	0.85015(20)	0.22533(7)	1.85(7)
C31	0.44428(19)	0.8224(3)	0.27003(9)	1.42(9)
C32	0.46552(20)	0.7261(3)	0.29179(9)	1.52(9)
C33	0.41195(21)	0.7011(3)	0.33553(10)	1.84(10)
C35	0.32057(20)	0.8631(3)	0.33560(10)	1.77(10)
C36	0.37255(19)	0.89233(25)	0.29155(10)	1.49(9)
C38	0.54636(21)	0.6504(3)	0.27012(10)	1.71(10)
O 4	0.69978(14)	0.78990(21)	0.23161(7)	1.92(7)
C41	0.73002(21)	0.7369(3)	0.27389(9)	1.52(9)
C42	0.83057(20)	0.7534(3)	0.29613(9)	1.47(9)
C43	0.85850(20)	0.6912(3)	0.33673(10)	1.57(9)
C44	0.79066(20)	0.6161(3)	0.35617(10)	1.58(9)
C45	0.68921(19)	0.60554(25)	0.33379(10)	1.56(9)
C46	0.65807(19)	0.6640(3)	0.29291(10)	1.58(9)
C47	0.81998(21)	0.5460(3)	0.40054(10)	1.91(10)
C48	0.90828(20)	0.8361(3)	0.27714(10)	1.58(10)
T11	1.07096(22)	1.0466(3)	0.42534(11)	2.37(11)
T12	1.04917(22)	1.2204(3)	0.38745(10)	2.21(10)
T13	0.91041(24)	1.1527(3)	0.44678(11)	2.32(11)
T41	0.93650(23)	0.5611(3)	0.41762(12)	2.78(12)
T42	0.74421(24)	0.5688(3)	0.44433(11)	2.79(12)
T43	0.80719(24)	0.4324(3)	0.38491(12)	2.58(12)
O 5	0.86224(20)	0.9026(3)	0.51497(10)	4.28(11)
O 6	0.89929(20)	0.8211(3)	0.44647(13)	5.06(14)
N 1	0.83913(21)	0.8741(3)	0.47299(11)	3.01(12)
CN1	0.73554(23)	0.9052(3)	0.45202(11)	2.16(10)
CN2	0.6674(3)	0.9649(3)	0.48111(11)	2.71(12)
CN3	0.5702(3)	0.9940(3)	0.46173(13)	3.57(14)
CN4	0.5408(3)	0.9654(3)	0.41399(14)	3.63(14)
CN5	0.6096(3)	0.9066(3)	0.38547(13)	3.98(16)
CN6	0.7085(3)	0.8748(3)	0.40444(13)	3.47(14)
C37	0.28288(18)	0.7303(3)	0.40709(8)	2.37(18)
C34	0.3370(3)	0.7678(4)	0.35872(10)	1.84(13)
TA 1	0.36941(25)	0.7067(3)	0.44648(12)	3.36(18)
TA 2	0.21772(25)	0.6319(3)	0.39625(13)	3.04(16)
TA 4	0.2074(3)	0.8150(3)	0.42688(14)	4.12(21)
C37A	0.2726(8)	0.7513(9)	0.4052(3)	2.7(7)
C34A	0.3422(12)	0.7716(14)	0.3588(4)	1.9(5)
TA1A	0.3027(15)	0.6461(10)	0.4280(6)	6.2(12)
TA2A	0.1533(8)	0.7505(15)	0.3902(6)	4.9(10)
TA4A	0.2920(13)	0.8371(11)	0.4439(5)	4.2(8)
C27	0.4208(3)	1.2786(3)	0.39837(17)	1.80(2)
C24	0.4634(6)	1.2129(6)	0.3548(3)	1.73(18)
TB 2	0.3397(4)	1.3582(4)	0.37844(18)	2.98(24)
TB 3	0.5150(4)	1.3351(6)	0.42359(24)	4.8(4)
TB 1	0.3650(6)	1.2081(5)	0.4367(3)	3.0(3)
C27A	0.4427(6)	1.2788(5)	0.3964(3)	2.1(3)
C24A	0.4714(10)	1.2105(8)	0.3513(4)	1.92(19)
TB 4	0.4247(9)	1.3905(6)	0.3787(3)	5.2(5)
TC 3	0.5353(7)	1.2761(7)	0.4344(3)	3.8(4)
TC 2	0.3395(7)	1.2380(9)	0.4211(5)	6.0(7)

[a] $B_{iso} = 8/3\pi^2\sum\sum U_{ij}a_i^*a_j^*(a_i \cdot a_j)$.

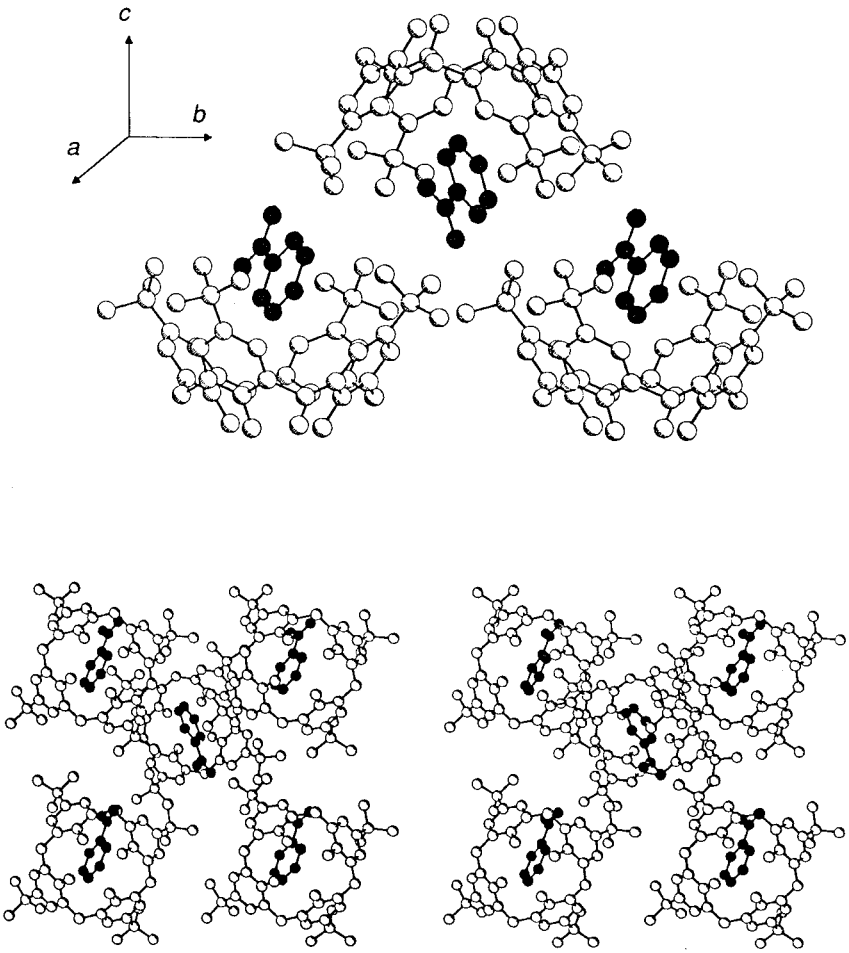

Figure 3. Packing arrangements of α-tBC·NB. Top: View of the bilayer packing. Bottom: Stereoview of the bilayer structure along the *c*-axis. The guest molecules are darkened for clarity.

(b) *p-tert*-Butylcalix[4]arene·Guest, Guest = 3- and 4-Nitrotoluene. In light of the 4-fold symmetric tBC·toluene and the asymmetric α-tBC·NB structures, it was of interest to see which ring substituent—methyl or nitro—would be more effective in directing the symmetry of the host·guest compound. The ^{13}C CP-MAS NMR spectrum of tBC·4-nitrotoluene (4NT) shows a deviation from 4-fold symmetry (Figure 4), but not to the extent seen for α-tBC·NB. The doublet carbon 7 host resonance suggests two possibilities: (i) the calix is 2-fold symmetric (like the low-temperature tBC·toluene structure) or (ii) the host:guest ratio is 2:1 (as in the tBC·anisole structure[3]) and the host is 4-fold symmetric. Although carbon intensities are not quantitative, the ratio of the host:guest lines are similar to the tBC·NB ^{13}C NMR spectrum and favor the former possibility. The guest methyl chemical shift value for tBC·4NT differs from that of the free guest by −6.4 ppm (Table 4). Since similar complexation-induced chemical shift (CIS) values are seen for tBC·toluene[1] and tBC·anisole,[15] the methyl group likely sits deep in the cavity with the nitro group protruding. The tBC·4NT structure then is one in which the guest methyl group is inserted into a 2-fold symmetric calix cavity.

In α-tBC·NB the nitrobenzene *meta* hydrogen is deep in an asymmetric calix cavity. If this guest orientation is directed by the nitro group and if the methyl group prefers to be deep in a symmetric cavity, 3-nitrotoluene (3NT) should satisfy both orienting criteria. The ^{13}C CP-MAS NMR spectrum of tBC·3NT is the most complex spectrum of the three asymmetric calix compounds (Figure 4). As with the spectrum of α-tBC·NB, the calix lines show the absence of any symmetry, and this suggests that each *tert*-butylphenol unit is unique (C7, $\delta = 33$ ppm). However, the *tert*-butylmethyl signals (C8) show a higher multiplicity than observed for the other two spectra, which suggests that there is a significant distortion of the *tert*-butyl groups of the calix. The presence of two sets of guest lines

(15) Brouwer, E. B. Ph.D. Thesis, Carleton University, Ottawa, Canada, 1996.

Table 4. ^{13}C CP-MAS NMR Spectral Data for α-tBC·NB, tBC·3NT, and tBC·4NT[a]

guest	carbon	calix[b]	solution[c]	**CIS**[d]
nitrobenzene	C-2	123.4	124.2	−0.8
	C-3	126.1	129.8	−3.7
	C-4	134.7	134.7	0.0
	C-1	*e*	149.1	*e*
4-nitrotoluene	Me	15.0	21.4	−6.4
	C-3	123.1	123.5	−0.4
	C-2	*e*	130.0	*e*
	C-4	145.8	146.2	−0.4
	C-1	149.2	146.2	+3.0
3-nitrotoluene	Me	13.9	20.2	−6.3
	Me′	17.2	20.2	−3.0
	C-5	120.1	119.9	+0.2
	C-6	*e*	123.0	*e*
	C-4	*e*	128.5	*e*
	C-2	133.7	134.8	−1.1
	C-1	140.5	139.3	+1.2
	C-3	147.5	147.5	0.0
	C-3′	148.5	147.5	+1.0

[a] All values in ppm. [b] Referenced to hexamethylbenzene (δ 16.9 ppm). [c] $CDCl_3$ solvent (from: Breitmaier, E.; Voelter, W.; *^{13}C NMR Spectroscopy*, 2nd ed.; Verlag Chemie: Weinheim, 1978) or spectra collected on a Bruker 300MSL spectrometer. [d] CIS = complexation-induced chemical shift = $\Delta\delta = \delta$(calixarene) − δ(solution). [e] Not observed.

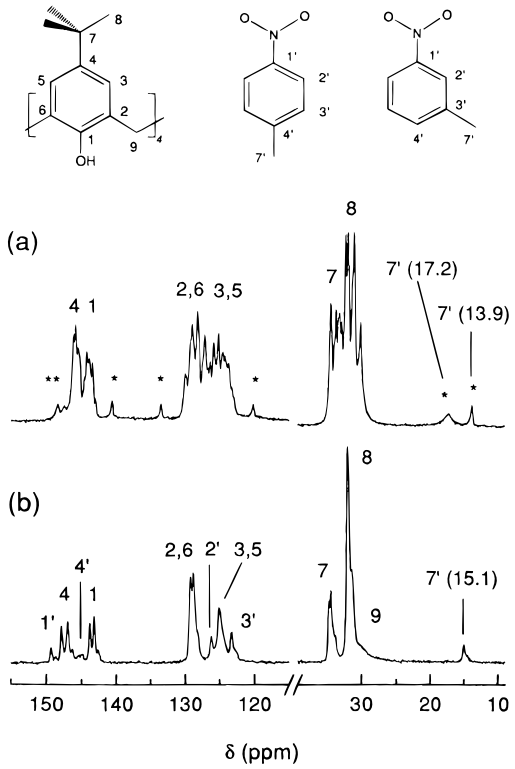

Figure 4. 45.3-MHz ^{13}C CP-MAS NMR spectra of (a) tBC·3NT and (b) tBC·4NT. Collection details: recycle time = 3.5 s; $\pi/2$ pulse = 2.8 μs; contact time = 3.5 ms; 4K datum points acquired and zero-filled to 16 K before processing; (a) 800 transients, ν = 3.14 kHz; (b) 700 transients, ν = 3.05 kHz. Starred lines indicate unassigned guest resonances.

(methyl: δ 17.2 ppm, broad; δ 13.9 ppm, narrow) suggests that, as for the toluene guest in the calix cavity,[1] there are two orientations of the guest methyl group in the host cavity (inserted and inverted). The methyl carbon experiencing the greatest amount of shielding (δ 13.9 ppm; CIS = −6.3 ppm) corresponds to the one inserted into the cavity. The other methyl oriented away from the calix cavity has a CIS value closer to that of the liquid (CIS = −3.0 ppm). Attempts to obtain single crystals of either compound suitable for X-ray crystallography were unsuccessful.

(c) Structure of *β*-*p*-*tert*-Butylcalix[4]arene·Nitrobenzene$_x$·-Propane$_y$ (*β*-tBC·NB$_x$·PROP$_y$; $x = 0.64$, $y = 0.36$, $x + y \leq 1$). The single-crystal XRD structure of tBC·NB$_x$·PROP$_y$, x = 0.64, y = 0.36 (Tables 2 and 5), reveals that both nitrobenzene (64%) and propane (36%) lie with their long molecular axes nearly coincident with the compound 4-fold axis although the propane position is poorly defined. The XRD structure shows no disordering in the host *tert*-butylphenol groups. Figure 2b shows the majority guest occupying an axial position in a C_4-symmetrical cavity, and it is positioned with the nitro group out of the cavity; this is the β-structural arrangement of tBC·-NB. The minority guest (not shown) also lies along the symmetry axis, with the methyl groups coincident with the on-axis nitrobenzene carbons C1′ and C4′. In contrast to the α-tBC·NB structure, the β-tBC·NB structure has a large *R*-factor, due in part to the inability to model the minority component which, because of its small size, is likely highly disordered in the cavity in addition to disordering about the 4-fold symmetry axis. Furthermore, propane is dynamic, as the −CH_2− resonance persists under ^{13}C CP-MAS NMR dipolar-dephasing conditions. For the crystallographic determination, overlap of the propane methyl groups with the axial nitrobenzene carbons is an additional complicating factor. Nevertheless, the structure unambiguously defines the nitrobenzene and propane guests as occupying axial positions in a symmetric cavity.

Table 5. Final Positional and Equivalent Isotropic Thermal Parameters (Å^2) for β-tBC·NB$_{0.64}$·PROP$_{0.36}$

atom	x	y	z	B_{iso}[a]
O1	0.6893(3)	0.6174(3)	0.06123(23)	4.38(17)
C2	0.7336(4)	0.5018(4)	−0.0777(4)	3.93(23)
C6	0.5651(4)	0.5837(4)	−0.0777(3)	3.91(23)
C5	0.5398(4)	0.5277(4)	−0.1709(4)	4.3(4)
C4	0.6073(4)	0.4598(4)	−0.2154(4)	4.5(3)
C1	0.6601(4)	0.5678(4)	−0.0344(4)	3.80(23)
C8	0.8398(4)	0.4866(4)	−0.0335(4)	4.22(24)
C3	0.7031(4)	0.4473(4)	−0.1689(4)	4.15(24)
C7	0.5801(5)	0.3947(6)	−0.3156(5)	6.3(3)
CT1	0.6627(6)	0.4106(7)	−0.4001(6)	8.2(5)
CT2	0.5725(6)	0.2808(6)	−0.2849(6)	7.2(4)
CT3	0.4774(7)	0.4284(8)	−0.3634(5)	10.0(5)
NNB	0.749(3)	0.7658(14)	−0.6294(8)	6.9(20)
ONB1	0.746(4)	0.6821(18)	−0.6752(9)	9.5(21)
ONB2	0.754(3)	0.8491(18)	−0.6757(15)	18.0(34)
CNB1	0.7453(19)	0.7663(9)	−0.5132(8)	3.7(27)
CNB2	0.739(3)	0.6734(11)	−0.4597(10)	7.3(22)
CNB3	0.736(3)	0.6739(19)	−0.3499(10)	23.3(31)
CNB4	0.739(3)	0.7672(24)	−0.2953(8)	4.4(33)
CNB5	0.745(3)	0.8601(19)	−0.3505(15)	16.5(58)
CNB6	0.7484(21)	0.8596(11)	−0.4602(15)	7.2(23)
CP1	0.755(12)	0.713(3)	−0.258(3)	4.5(13)
CP2	0.767(13)	0.677(4)	−0.373(4)	12.0(37)
CP3	0.787(4)	0.771(6)	−0.445(3)	3.4(11)

[a] $B_{iso} = 8/3\pi^2\sum\sum U_{ij}a_i^*a_j^*(a_i\cdot a_j)$; B_{iso} is the mean of the principal axes of the thermal ellipsoid. ESD's refer to the last digit printed.

Nitrobenzene sits 4.49 Å above the basal plane defined by the four phenolic oxygens. Contacts near the sum of the van der Waals radii (3.6 Å) between guest and host include the following: CNB3···tBuMe (3.62 Å), CNB2···C5 (3.74 Å), CNB6···C3 (3.89 Å).The guest CNB4 approaches the host C1, C2, and C6 with distances of 4.30, 4.26, and 4.39 Å.

(d) Tuning of the Nitrobenzene Orientation in the Calix Cavity. The nitrobenzene orientation in the calix cavity as well as the tBC·guest symmetry can be tuned by incorporation of propane as a second guest. As the propane pressure, P_{PROP}, increases during the preparation of tBC·NB$_x$·PROP$_y$ (where $x + y \leq 1$) propane is incorporated in increasing amounts and the nitrobenzene guest is aligned with the calix symmetry axis.

^{13}C CP-MAS NMR spectra of tBC·NB$_x$·PROP$_y$ (where $x + y \leq 1$) monitor the transition in structures from asymmetric to C_2 symmetric, and finally to C_4 symmetric (Figure 5). In the first transition, the nitrobenzene orientation changes from a non-axial position to an axial one in which the nitrobenzene molecular axis is coincident with the calix symmetry axis. The off-axis α-tBC·NB structure persists when synthesized under P_{PROP} = 15 psi (Figure 5a), and the ^{13}C NMR spectrum is identical with that of α-tBC·NB (Figure 1). Preparation under P_{PROP} = 20 psi (Figure 5b) gives a compound that incorporates a small amount of the second guest (δ = 14, 16 ppm) and shows two nitrobenzene orientations as identified by the nitrobenzene C-3′ resonances at δ = 123.4 and 121.9 ppm. The former line arises from the nitrobenzene in the non-axial position, while the latter corresponds to the axial guest. With 20 psi < P_{PROP} < 100 psi, the product (Figure 5c) is solely the β-tBC·NB$_x$·-PROP$_y$ compound with incorporation of propane and nitrobenzene in the axial orientation, as determined by the XRD structure. Finally, under higher propane pressures (175 psi), no propane is incorporated in the solid product, which shows a ^{13}C NMR spectrum typical of a C_4-symmetric compound (Figure 5d). The crystal used for the crystallographic determination gave a ^{13}C NMR spectrum identical with spectrum c.

Table 6. ^{2}H NMR Spectral Parameters[a]

material	*T*/K	$\Delta\nu_{xx}$/kHz	$\Delta\nu_{yy}$/kHz	$\Delta\nu_{zz}$/kHz	χ/kHz	η
NB-d_5	77	266[b,c]	137	129	177.3	0.030 ± 0.011
α-tBC·NB-d_5	200	258[b,c]	134	124	172.0	0.038 ± 0.012
α-tBC·NB-d_5	290	158[b]	133	25	105.3	0.684 ± 0.025
		252[c]	134	118	168.0	0.063 ± 0.012
tBC·(NB-d_5)$_x$·PROP$_y$	136	162	131	31	108.0	0.617 ± 0.024

[a] Estimated errors of ±1.5 kHz in the measurements of the $\Delta\nu_{ii}$ and ±1 kHz in χ. [b] For the *ortho*, *meta* deuterons. [c] For the *para* deuteron.

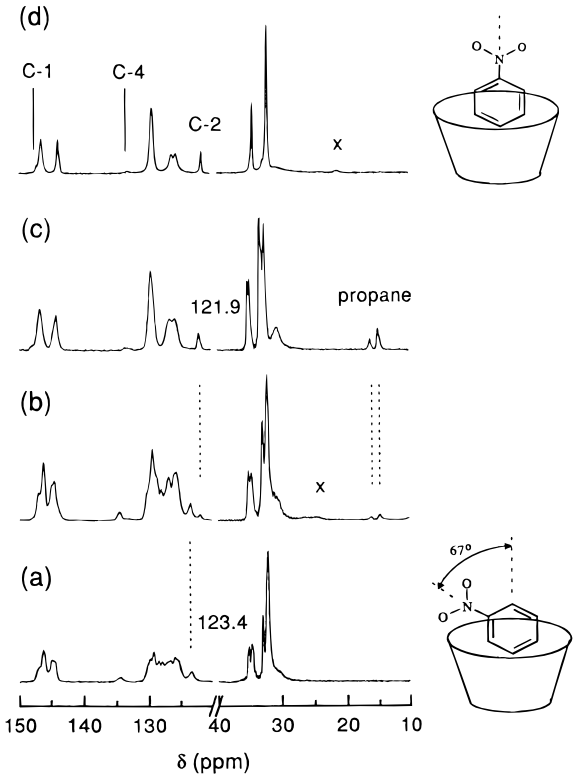

Figure 5. ^{13}C CP-MAS NMR spectra of tBC·NB$_x$·PROP$_y$ (where $x + y \leq 1$) compounds prepared with an overpressure of propane: (a) 15 psi, $x = 1$; (b) 20 psi; (c) 100 psi; (d) 175 psi, $x = 0$. Collection details: (a−c) at 45.3 MHz, 800−3500 transients, recycle time = 4 s, $\pi/2$ pulse = 3.5 μs, contact time = 3.5 ms, 3 K data points acquired and zero-filled to 8 K before processing, SW = 20 kHz, $\nu = 2.9-3.2$ kHz; (d) at 75.5 MHz, 750 transients, recycle time = 3 s, $\pi/2$ pulse = 3.9 μs, contact time = 3.0 ms, 6K datum points acquired and zero-filled to 16K before processing, SW = 30 kHz, $\nu = 4.62$ kHz.

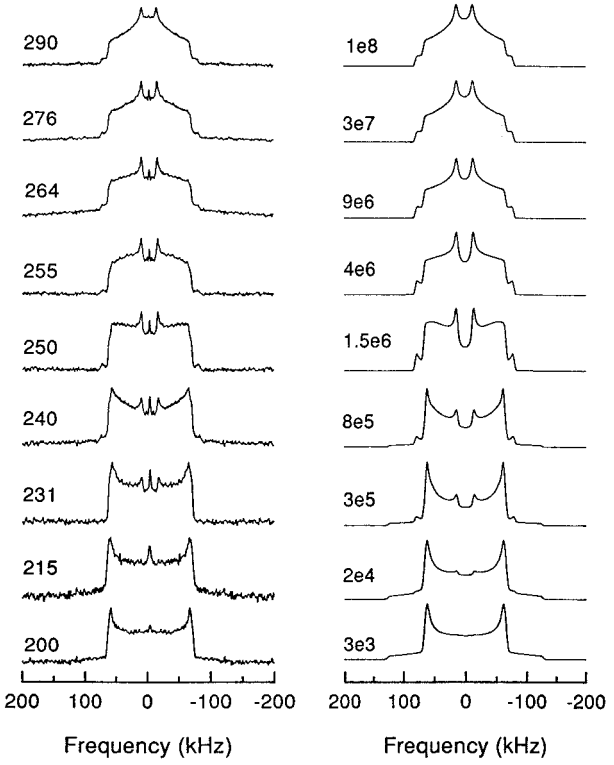

Figure 6. Observed (left) and simulated (right) 46.1-MHz ^{2}H NMR spectra of α-tBC·NB-d_5; collection temperatures (K) and jump rates κ (Hz) are indicated above each spectrum. Collection details: 400 scans; recycle time = 5 s; $\pi/2$ pulse = 2.5 μs; echo delay = 35 μs; line broadening = 500 Hz; 512 datum points acquired and zero-filled to 1K before processing.

The nitrobenzene carbon 2′ resonance is the guest signal most sensitive to the guest orientation and the ^{13}C NMR spectrum b clearly shows the presence of two nitrobenzene orientations. The other guest carbon resonances are invariant (4′, $\delta = 134.7$ ppm) or are partially (1′, $\delta = 147.2$ ppm) or fully obscured (3′) by the calixarene aromatic carbon resonances. The upfield shift in the 2′ resonance indicates that this carbon moves closer to the aromatic walls of the calix cavity as the guest adopts the axial position.

The tBC carbon lines become sharper as P_{PROP} increases, indicating that the cavity symmetry increases as the nitrobenzene guest becomes axial. In particular, the *tert*-butyl carbons 7 and 8 (δ 35, 33 ppm) are sharp 1:1 doublets (at $P_{PROP} = 100$ psi) which suggest that either the cavity has at most local 2-fold symmetry or each of the two guests influences its host cavity in a slightly different manner. Due to size and electrostatic differences, propane and nitrobenzene likely exert slightly different influences on their respective host cavities. Thus, the two resonances observed for each *tert*-butyl carbon resonance indicate two slightly different host geometries. This feature may account for the fit of the structure model to the diffraction data.

At higher P_{PROP}, propane is (surprisingly) absent from the β-tBC·NB lattice, which has an axial nitrobenzene and possesses C_4 symmetry. Finally, the downfield shift in the host aliphatic δ values with increasing P_{PROP} may result from the proximity of the guest nitro group to the host *tert*-butyl groups.

(e) ^{2}H NMR Studies of α-tBC·NB-d_5 and β-tBC·(NB-d_5)$_x$·PROP$_y$. Guests in the calixarene cavity undergo motion, even in the solid state. For both compounds, the ^{13}C CP-MAS dipolar-dephasing experiments suggest large-amplitude motion of the guest molecule with the C4′−H bond on the symmetry axis for the motion.

Additional dynamic information comes from ^{2}H NMR spectroscopy. Figure 6 shows the experimental and simulated ^{2}H NMR spectrum of the low-symmetry α-tBC·NB-d_5 compound from 200 to 290 K. The 290 K spectrum is typical of a 2-fold axial rotor in the fast motion limit (FML).[16] Spectra taken at lower temperatures reflect the decrease in frequency of this motion, κ, until 200 K, where the guest motion is frozen in. Examination of the static and FML line shapes gives the components of the static and FML tensors (Table 6). The calculated angle for the C−D bond (with respect to the long molecular axis) is 59.6°, slightly less than the expected 60°.

(16) Gall, C. M.; DiVerdi, J. A.; Opella, S. J. *J. Am. Chem. Soc.* **1981**, *103*, 5039−3043.

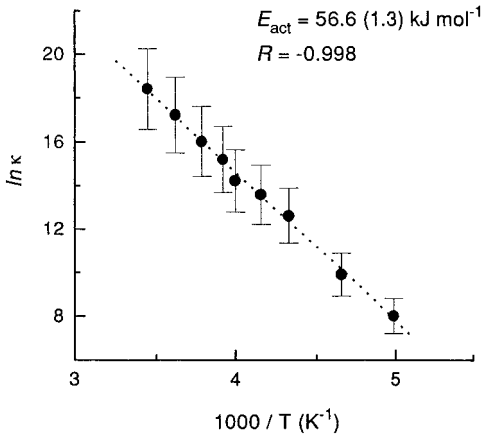

Figure 7. Arrhenius plot of ln κ against inverse temperature for α-tBC·NB-d_5.

The line shapes were simulated by using the static line-shape parameters and a model chosen in which the nitrobenzene undergoes a 2-fold jump about its long molecular axis. The line shape is a sum of contributions from the *para* deuteron on-axis component (invariant with motion) and the *ortho* and *meta* deuterons (vary with motion). The frequency of motion, κ, is correlated to temperature by visibly matching the simulated and observed spectra. An Arrhenius plot of ln κ against the inverse temperature gives a barrier to 2-fold ring flips of E_{act} = 56.6 ± 1.3 (±σ, n = 9) kJ mol^{-1} (Figure 7).

The barrier to 2-fold rotation of the nitrobenzene is much larger that observed for the 2-fold jump of the guest in tBC·-toluene-d_5 (E_{act} = 34 ± 3 (±σ, n = 7) kJ mol^{-1}).[1] The difference is likely related to the inability of the nitrobenzene guest to match the host symmetry, which is in turn related to the difference in position of the two guests (the axis of toluene motion is coincident with the tBC 4-fold symmetric axis whereas the rotation axis of the nitrobenzene is 67.9° off the tBC *z*-axis). The latter structure shows the aromatic ring of the guest wedged between two *tert*-butylphenol units, which raises the barrier to the jumping motion compared to the toluene which occupies a more open (and energetically less restricted) position in the calix cavity.

A consequence of axial *vs* non-axial guest position in the calix cavity is illustrated by the ^{2}H NMR spectra of the high-symmetry β-tBC·(NB-d_5)$_x$·PROP$_y$ in which the nitrobenzene occupies an axial position (Figure 8). The 136 K spectrum has the distinctive 2-fold FML line shape (Table 6).[16] In contrast to the α-tBC·NB-d_5, in which the nitrobenzene is in an off-axis position, the axially-positioned nitrobenzene is already undergoing rapid 2-fold flips below the temperature at which the non-axial nitrobenzene even begins to show dynamic effects ($\kappa < 10^3$ Hz; static line at 200 K). The axially-positioned guest thus experiences a significantly lower barrier to rotation.

The axial nitrobenzene-d_5 line shapes narrow further at higher temperatures, and show the gross features consistent with 4-fold motion. However, two factors (also seen with tBC·toluene-d_5) hinder a more quantitative treatment of the ^{2}H NMR data: First, the FML for the motional narrowing is not reached by the maximum temperature of 319 K; the FML line shape is key for selecting a motional model. Secondly, the broadened features suggest the presence of a distribution of motional rates, which complicate the line shape intensity distribution with the simulated line shapes. Consequently, these data were not simulated.

(f) Double Guests and the Host Lattice. Several structural motifs occur with the compounds of tBC with nitrobenzene and small gas molecules (propane as well as methane,[15] ethane,[15] ethylene,[15] butane[15] and xenon[17]) as the major and minor guests, respectively. The α- and β-tBC·NB structural motifs differ in the major guest orientation as well as compound symmetry. The quantity rather than the exact nature of the minor guest appears to be crucial in directing which structure the resulting compound will adopt. That the tBC structure is very sensitive to the presence of the second guest indicates the importance of long-range intermolecular host·guest interactions.

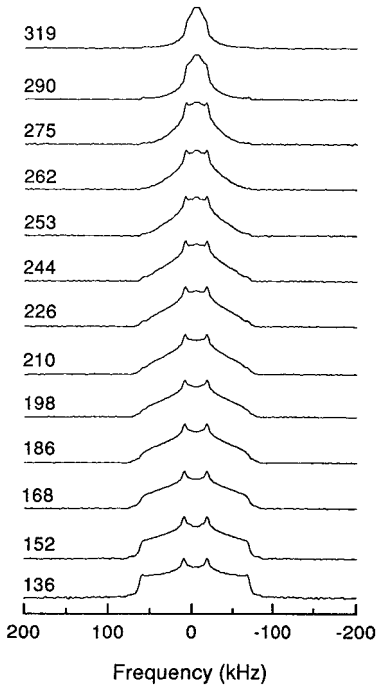

Figure 8. Variable-temperature (in K) 46.1-MHz ^{2}H NMR spectra of β-tBC·(NB-d_5)$_x$·PROP$_y$. Collection details: 200 transients; recycle time = 8−15 s; π/2 pulse = 2.6 μs; sweep width = 1.25 MHz; echo delay = 35 μs; 0.2 kHz line broadening; 1K datum points acquired and zero-filled to 2K before processing.

Interactions between nitrobenzene guests appear to direct the guest orientation (and the overall compound symmetry) in α-tBC·NB. Nitrobenzene molecules (large dipole moment μ = 3.6 D) pole in the *ab* plane and cause a net dipole moment in the non-centrosymmetric α-tBC·NB crystal. In contrast, the nitrobenzene dipole moments, now aligned along the symmetry axis, cancel in the centrosymmetric β-tBC·NB$_x$·PROP$_y$ crystal, and consequently, this compound does not have a net dipole moment. In the high-symmetry case, the nitrobenzene guest−guest interaction (the smallest distance between guest nitrogens is 8.93 Å) no longer directs the guest orientation and compound symmetry; these features may arise from other interactions such as crystal packing forces which become prominent as substitution of nitrobenzene by propane disrupts nitrobenzene guest−guest interactions.

Translational ordering of tBC·guest compounds arises from a repeatable orientation of the guest in a calix cavity: each guest must sit in an identical position in a calix cavity that has a shape that persists throughout the lattice. Since the guest environment is defined by several calixarene molecules, the long-range ordering is propagated (in part) by the guest orientation. Defect sites arise when either one guest adopts an alternative orientation or a cavity is occupied by a second guest (and the long-range ordering is broken).

The tBC·NB structure appears to be insensitive to the presence of a small fraction of a second guest. However, as

(17) Brouwer, E. B.; Enright, G. D.; Ripmeester, J. A. *Chem. Commun.* **1997**, in press.

the number of defect sites increases (with an increase in the fraction of propane), the off-axis nitrobenzene orientation and the host symmetry are no longer propagated through the lattice, and an axial nitrobenzene orientation and a higher host symmetry are adopted. It is surprising then that the C_4 symmetric β-tBC·NB_x (where $x \leq 1$) contains no propane (Figure 5d), despite its preparation under a high pressure of propane (175 psi). It is likely that during crystallization, propane initially occupies a large enough fraction of host cavities to cause nitrobenzene in the remaining calix cavities to adopt an axial orientation and the compound to have C_4 symmetry. Cavity-to-cavity and out-migration of propane from calix cavities occurs as a consequence of these structural changes. The high-symmetry β-structure is unable to incarcerate the second guest as tightly as in the α-structure, and subsequent to the formation of β-tBC·NB_x·$PROP_y$, the propane migrates out of the lattice.

Two features—the lower packing density in the *P*4/*n* space group relative to $Pc2_1/n$ and a significant decrease in the number of nitrobenzene guests concomitant with the increase in the number of propane guests—increase the interstitial void spaces in the crystal and permit the departure of propane. The calixarene bilayer separation increases as the space group changes from $Pc2_1n$ to *P*4/*n* and thus the interstitial void space increases. Furthermore, the nitrobenzene guest may act as a gate to propane site-to-site migration: when it is in the off-axis position (the low-symmetry α-structure), the interstitial channels are both small and closed, but when the nitrobenzene is in the on-axis position (the high-symmetry β-structure), the interstitial channels are large and opened. Finally, it is anticipated that the absolute number of nitrobenzene molecules is important in controlling the migration of propane. It is expected that the β-tBC·NB lattice contains a large number of empty calix cavities due to the small fraction of remaining cavities occupied by nitrobenzene. Departure of propane from the lattice is not unexpected in light of the penetration of the empty solid tBC lattice by liquid propane to give a C_4-symmetric structure (Figure 9). The mostly empty β-tBC·NB_x (where $x \leq 1$) lattice may be microporous, and possess structural characteristics of pillared materials such as clays.[18]

The NMR and XRD studies of the tBC·NB_x·$PROP_y$ compound serve to bridge solid-state and solution studies. As the number of defects increases in the tBC·NB_x·$PROP_y$ lattice, a molecular interpretation becomes more appropriate as a distribution of the defect sites throughout the crystal will give rise to localized difference; this description is analogous to a description of solutions. However, as the number of defects in the tBC·NB_x·$PROP_y$ lattice decreases, a lattice interpretation is more suitable.

Summary

Despite the preference of the *p-tert*-butylcalix[4]arene host for forming C_4-symmetric compounds with small guests, nitrobenzene and related guests give a compound where the calix has no symmetry elements. tBC compounds with both nitrobenzene and propane guest molecules show that the asymmetric α-tBC·NB structural motif is favored at low occupancy of the second gas, but as the fraction of cavities occupied by the gas molecule increases, the compound structure becomes symmetric, and the nitrobenzene molecular axis is aligned with the host symmetry axis. The position of the major guest and the compound symmetry are tunable with the presence of the minor guest.

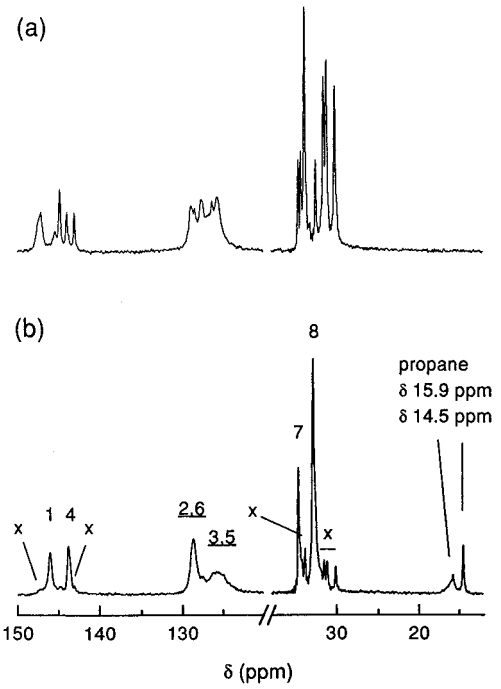

Figure 9. 75.4-MHz ^{13}C CP-MAS NMR spectra of (a) empty tBC and (b) tBC·propane at 290 K. The guest assignments are indicated, and the host assignments are as in Figure 1; × = empty tBC. Collection details: 700 transients; recycle time = 5 s; $\pi/2$ pulse = 5.5 μs; contact time = 4 ms; 6K datum points acquired and zero-filled to 16K before processing; SW = 30 kHz; ν = 4.1 kHz.

The processes of crystal nucleation and propagation must be considered in order to understand fully the relationship between the two guests and the host in the crystalline lattice. Fundamental questions arising from this work will need to be addressed. In particular, which species is initially nucleated—tBC·nitrobenzene or tBC·propane? The synthesis of tBC·pentane and tBC·cyclohexane by the vapor diffusion method shows that in some cases, tBC·NB does not crystallize at all,[19] whereas with propane, the vast majority of calix cavities are occupied by nitrobenzene. The species that nucleates first may do so as a function of solubility of the host·guest compound: tBC is less soluble in aliphatic hydrocarbons than it is in nitrobenzene. It may be that both species nucleate, and the resulting structure is determined by the process of crystal growth. Once nucleation has occurred, does one guest preferentially incorporate into the growing lattice? Does guest migration take place? Is the rate of crystal growth more significant than the thermodynamic stability of the product under the synthesis conditions? Many questions need to be addressed to fully understand the structure and behavior of this system.

Acknowledgment. We thank the Natural Sciences and Engineering Research Council of Canada for support in the form of operating (J.A.R.) and post-graduate PGS-B (E.B.B.) awards, as well as Xu Zhu for technical assistance.

Supporting Information Available: Listings of crystallographics data, atomic parameters, *U* values, distances, and angles (28 pages). See any current masthead page for ordering and Internet access instructions.

JA9637762

(18) Barrer, R. M. *J. Incl. Phenom.* **1986**, *4*, 109−120. Barrer, R. M. *Clays Clay Miner.* **1989**, *37*, 385−395. Chen, B. Y.; Kim, H.; Mahanti, S. D.; Pinnavaia, T. J.; Cai, Z. X. *J. Chem. Phys.* **1994**, *100*, 3872−3880.

(19) Brouwer, E. B.; Enright, G. D.; Ripmeester, J. A. *Supramol. Chem.* **1996**, *7*, 143−145.